

## A New Insight on $Pb(Mg_{1/3}Nb_{2/3})O_3$ Nano Scale Powders for Thin Film Capacitor

Mehmet Faruk EBEOĞLUGİL<sup>1</sup> and Erdal ÇELİK<sup>2,3,4</sup>

<sup>1</sup>Dumlupınar University, Engineering Faculty, Department of Material and Ceramic Engineering, Kutahya

<sup>2</sup>Dokuz Eylül University, Engineering Faculty, Department of Metallurgical and Materials Engineering, Buca, Izmir

<sup>3</sup>Dokuz Eylül University, Center for Production and Applications of Electronic Materials (EMUM), Buca, Izmir

<sup>4</sup>Dokuz Eylül University, Graduate School Natural and Applied Sciences, Nanoscience and Nanoengineering, Buca, Izmir  
e-posta: erdal.celik@deu.edu.tr

Geliş Tarihi:26.10.2012; Kabul Tarihi: 11.11.2013

### Abstract

The present paper extensively demonstrates synthesis, characterization and electrical properties of relaxor ferroelectric  $Pb(Mg_{1/3}Nb_{2/3})O_3$  (PMN) nano scale powders and PMN thin films on n-type Si substrates using sol-gel technique for capacitor applications. Transparent solutions were prepared from Pb, Mg and Nb based precursors, methanol and glacial acetic acid (GAA). The obtained solutions were dried at 80°C for 60 minutes in air to form gel structure of PMN mixture and heat treated at 530°C for 3 hours and subsequently sintered at the temperature range of 800 °C and 1000°C for 2 hours in air. After the sintering, the PMN powders were milled for 24 hours to obtain nano scale powders. The powder size was measured using particle size machine. Finally the powders were dispersed in alcohol and the obtained suspension was coated on n-type Si substrates. The films were dried at 50°C for 15 minutes and subsequently were heat treated at 730 °C for 30 minutes in air to ensure its adhesion strength. Thermal, structural, microstructural, mechanical and electrical properties of the powder and the coatings were characterized by DTA/TG, FTIR, XRD, SEM, refractometer, spectrophotometer and high resolution dielectric analyzer machines. The study provides a new insight on the nano scale powders of PMN structure coated on Si semiconducting surface.

### Key words

PMN; Nano powder;  
Capacitance; Dielectric;  
Thin film

## İnce Film Kapasitör İçin $Pb(Mg_{1/3}Nb_{2/3})O_3$ Nano Ölçekli Tozlar Hakkında Bir Yeni Anlayış

### Özet

Mevcut makale kapasitör uygulaması için sol-jel tekniği kullanılarak relaksör ferroelektrik  $Pb(Mg_{1/3}Nb_{2/3})O_3$  (PMN) nanotozların ve n-tipi Si altlıklar üzerine PMN filmlerin sentezlenmesi, karakterizasyonu ve elektriksel özellikleri geniş bir şekilde açıklanmaktadır. Saydam çözeltiler Pb, Mg ve Nb esaslı prekürsörler, metanol ve glasiyel asetik asitten (GAA) hazırlanmıştır. Elde edilen çözeltiler PMN karışımın jel yapısını oluşturmada 80°C'de 60 için havada kurutulmuş ve 530°C'de 3 saat için ısı işlem yapılmış ve bunu takiben 800 °C ve 1000°C aralığında 2 saat için havada sinterlemiştir. Sinterleme sonrası PMN tozları nano ölçekli toz oluşturmak için 24 saat öğütülmüştür. Toz boyutu partikül boyut ölçüm cihazıyla ölçülmüştür. Sonuçta tozlar alkolde disperse edilmiş ve oluturulan süspansiyon n-tipi Si üzerine kaplanmıştır. Filmler 50°C'de 15 dakika için kurutulmuş ve müteakiben bunların yapışma mukavemetini artırmak için 730 °C'de 30 dakika için havada ısı işlem yapılmıştır. Tozların ve kaplamaların termal, yapısal, mikroyapısal, mekanik ve elektriksel özellikleri DTA/TG, FTIR, XRD, SEM, refraktometre, spektrofotometre ve yüksek çözünürlüklü dielektrik analizör cihazları kullanılarak karakterize edilmiştir. Çalışma Si yarıiletken yüzey üzerine kaplanmış PMN yapısının tozlardan oluşturulması bir yeni anlayış sağlamıştır.

### Anahtar kelimeler

PMN; Nano toz;  
Kapasitans; Dielektrik;  
İnce film

© Afyon Kocatepe Üniversitesi

### 1. Introduction

Lead magnesium niobate,  $Pb(Mg_{1/3}Nb_{2/3})O_3$  (PMN) ferroelectric relaxor have so far attracted considerable attention from numerous researchers

due to its desirable properties such as high dielectric constant which can be used in applications such as capacitors and actuators (Schwartz, 1997). The dielectric constant, however,

was found to be considerably lowered in the occurrence of pyrochlore phase (Parola, *et al.* 2003). PMN nano-powders have become highly important with their cubic perovskite structure and better dispersion and dielectric characteristics. The sol-gel process, which offers simple and low-cost processing, is adopted extensively to synthesize nano-powders in laboratory and industry. Compared to the solid-reaction method, the sol-gel process possesses better control the stoichiometry of the powders, and permits doping with different additives in addition to the high purity and uniform structure of the product (Guha, 1999; Bhuiyan, *et.al.* 2006.).

Much of the works reported, therefore, have been on the processing of pyrochlore free PMN powders, whereas investigations on the effect of the powders on properties of ceramics have been found to be limited. Notwithstanding different synthetic routes of mixed oxides have been used to produce PMN powder, a particular milling time was used (Chaipanich and Tunkasiri, 2007). Little is known, however, on the effect of milling time on the properties of PMN ceramics. Earlier work by the authors (Chaipanich and Tunkasiri, 2007; Deliormanlı, *et.al.* 2007; Sakar-Deliormanlı, *et.al.* 2008; Sakar-Deliormanlı, *et.al.* 2009) has shown that an increase in the perovskite phase of PMN powder was found when the starting precursors,  $MgNb_2O_6$  and  $PbO$  were subjected to longer milling (Chaipanich and Tunkasiri, 2007). Nevertheless, it is not known the effect of these powders on the properties of ceramics. Therefore, the effects of milling time on the grain size and dielectric properties of PMN ceramics produced using  $Pb$ ,  $Mg$  and  $Nb$  based starting precursors, methanol and glacial acetic acid (GAA) were investigated in this research.

## 2. Material and Method

Sol-gel-derived nano-powders of PMN solutions were prepared from lead acetate trihydrate ( $Pb(CH_3COO)_2 \cdot 3H_2O$ ), magnesium acetate tetrahydrate ( $Mg(CH_3COO)_2 \cdot 4H_2O$ ) and niobium ethoxide ( $Nb(OC_2H_5)_5$ ). The precursors were dissolved in methanol and glacial acetic acid. Here,

methanol and glacial acetic acid were used as solvent and chelating agent, respectively. Then, the prepared solutions were mixed in an open vessel kept at room temperature for 1 hour in air to gain transparent and homogeneous solutions. In order to determine solution characteristics, which affect thin film structure, turbidity, pH values, and rheological properties of the prepared solutions were respectively measured by turbidimeter, pH meter, and rheometer machines before coating process. Turbidity properties of the solutions were measured to use standard solutions for coating process by VELP TB1 Model turbidimeter. After preparation of transparent solutions, pH values of the solutions were measured to determine their acidic and basis characteristics using a standard pH meter with Mettler Toledo electrode. In addition to pH value and turbidity properties, rheological behavior of the solutions including viscosity and gel point was determined by CVO 100 Digital Rheometer (Bohlin Instrument).

The partially hydrolyzed solution was aged for a longtime in a drying cabinet at  $60^\circ$ – $80^\circ C$ . During this time, the solvent in the sol was evaporated in air and the three precursors reacted to form a solid gel. The solid gel was baked at a heating rate of  $10^\circ C \cdot min^{-1}$  in a box-type furnace, and finally annealed at  $500^\circ C$  for 3 hours in air. The powder was annealed in similar manner but at  $950^\circ C$  which was maintained for 2 hours.

Thermal behavior of PMN based powders, which was dried at  $150^\circ C$  for 30 minutes in air, was evaluated to gain decomposition and phase formation at a heating rate of  $10^\circ C/min$  under oxygen atmosphere by using DTA/TG machine (DTG-60H Shimadzu).  $Al_2O_3$  powder was used as a reference material. FTIR (Perkin Elmer) absorption spectra were measured over the range of  $4,000$ – $400\text{ cm}^{-1}$  at room temperature after the reactions in the temperature range of  $25^\circ C$  and  $600^\circ C$  for 30 minutes in air. After preparing powders at these temperatures, they were mixed with potassium bromide (KBr). All of these seven samples were characterized by FTIR. According to the results, depending on temperature, variation of organic

component's concentration can be determined by organometallic and polymer library supplied by Perkin Elmer. In order to optimize process conditions, the obtained results were commented, as a combination of DTA-TG and FT-IR analyses.

Mean particle size of calcined PMN powder was measured using Malvern Laser Mastersizer machine. Table 1 shows powder size of PMN powders after 12 hours ball milling. In general, particle size can be seen to reduce with increasing milling time. Measured mean particle size of the PMN powders after 12 hours was reduced from 68  $\mu\text{m}$  to 0.414  $\mu\text{m}$ . Again the powder was ground for a second time in order to guarantee uniform grain size. At last, "flaxen" PMN nano-powders (~200 nm), were collected by filter technology. The nano scale powders were used to prepare PMN thin films for capacitor applications.

**Table 1.** Powder size of PMN after 12 hours ball milling

Milling Time	d(0.1) $\mu\text{m}$	d(0.5) $\mu\text{m}$	d(0.9) $\mu\text{m}$
Starting	6,390	67,994	252,501
After 12 h	0,166	0,414	11,698

Due to the fact that lead volatilizes at 750°C, it was important to form the pyrochlore phase. Excess lead (to the extent of 10 mole %) was added into the starting precursor solution to compensate for the lead loss during heating. The crystal characteristics of PMN powders were analyzed by XRD with  $\text{Cu-K}\alpha$  radiation and a graphite monochromator with a  $2\theta$  range extending from 15° to 80°. A step scan with a step size of 0.02° and a counting time of 1 s/step was used.

Prior to the coating process, n-type Si substrates were rinsed in acetone using a standard ultrasonic cleaner and subsequently dried in air. The Si substrates were coated by the suspension having PMN nano scale powder mixed in 8 ml methanol. The deposited suspensions were dried at room temperature in air. We repeated this procedure for six cycles for each samples, after completing the drying of each coated samples. Finally the PMN coatings were heat treated at 750°C for 30 minutes in air to ensure adhesion strength.

The surface topographies of PMN films were examined by using SEM (JEOL JSM 6060).

Vacancies, micro cracks and porosities were examined by SEM in order to determine the effect of ball milling and grain size on the morphology of the thin films.

Optical properties of the produced films were evaluated using refractometer and spectrophotometer machines. Refractive indexes of thin films were measured at selected wavelengths in the VIS region by a high-accuracy Abbe refractometer at room temperature. Refractive indexes were used to determine film thickness using V-530 JASCO UV/VIS Spectrophotometer.

Dielectric constant of PMN thin film samples were measured using a high resolution dielectric analyzer (Novo Control, Alpha-N). For the measurements, silver (Ag) paste was applied to form metal oxide semiconductor (MOS) structure of the PMN films to improve the contact with the analyzer plates. A heat treatment at 300 °C was applied to the Ag paste coated samples for 30 minutes. Relative permittivity of the PMN samples was measured at room temperature as a function of frequency in the range  $10^{-1}$  Hz to  $10^7$  Hz. During the measurements AC volts (0.1 Vrms) was applied to the PMN thin film samples.

### 3. Results and Discussion

With turbidity experiments, whether powder precursor materials are dissolved very well in solutions is understood by looking ntu values before coating process. As mentioned before, turbidity values of solutions change in the range of 0 ntu and 1000 ntu. It is interpreted that powder based precursors are completely dissolved as turbidity value approaches to 0 ntu and they are not dissolved and some powder particles are suspended in a solution as it approaches to 1000 ntu. The fabrication of pure perovskite PMN powder or thin films is directly related to turbidity values of the solutions, which is 0 ntu. In this experiment, turbidity value of the solutions was measured as 8.42 ntu (Table 2). Based on the turbidity value, it can be pointed that powder based precursors are completely dissolved in the solutions. Moreover, these values present an important clue for further processing. It is worth

noticing that optimum structural, thermal, microstructural, mechanical, optical and high dielectric properties are not obtained using undissolved solutions.

Table 2 demonstrates pH values of the solutions depending on time. According to this result, it is clear that acidity of the solutions does not change with in first 15 minutes because it stabilizes. It was estimated that pH values are stable because of PMN precursor. Now that pH value of the solution is an important factor influencing the formation of the polymeric three- dimensional structure of the gel during the gelation process, it should be taken into consideration while preparing solutions. Whilst ramified structure is randomly formed in acidic conditions, separated clusters are formed from the solutions showing basic characters (Culha, et.al. 2009). The other factor is dilution of the solution using solvent. The excess solvent physically affects the structure of the gel, because the liquid phase mainly consists of the excess solvent during the aging procedures. The changes in the gel structure at this stage partly influence the final structure characters (Culha, et.al. 2009).

**Table 1.** Turbidity and pH values of the prepared solutions

Queue of measurement	Turbidity (ntu)	pH
After preparing solutions	8.26	5.85-6.00
After 5 minutes	8.45	5.85-6.00
After 10 minutes	8.47	5.85-6.00
After 15 minutes	8.51	5.85-6.00

Gelation occurs when aggregation of particles or molecules takes place in a liquid, under the action of Van der Waals forces or via the formation of covalent or no covalent bonds. The process can be investigated using rheological measurement techniques (Culha, et.al. 2009). Figures 1 and 2 show rheological properties such as viscosity, viscous and elastic modulus for the solutions prepared from 8 ml methanol as a function of temperature and time. Figure 2 depicts viscosity values of the solutions as a function of time at 25°C, 50°C and 80 °C for 9000 s in air. Viscosity values of the solutions at 25°C, 50°C and 80 °C

were found to be 0.26 mPa.s, 0.12 mPa.s and 4 mPa.s, respectively.

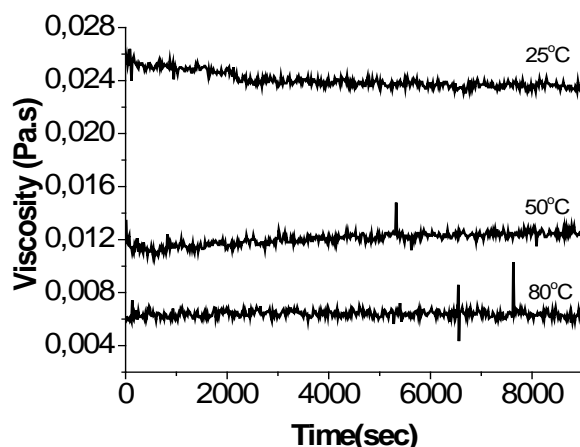


**Figure 1.** Viscosity values of the PMN based solutions at different temperature depending on time.

Insight into complex gelation mechanism can be gained from the following analysis having viscoelastic behaviors of the solution. Figure 2 denotes viscous and elastic moduli of the solution at 25°C, 50°C and 80 °C for 9000 s in air. Here, the experiment was performed at 25 °C for 3000 s and then at 50 °C for period between 3000 and 6000 s. After that, the experiment was completed at 80 °C for period between 6000 and 9000 s. As clearly seen from Figure 2, elastic and viscous moduli have an intersection point at 4703 s on x-axis. It can be indicated that viscous and elastic moduli can be changed depending on time and temperature for our cases. The time necessary to reach the intersection depends on the oscillations frequency ( $\omega$ ). Therefore, this intersection could be used to define the experimental gel point (Pierre and Bernard-Lyon, 1998).

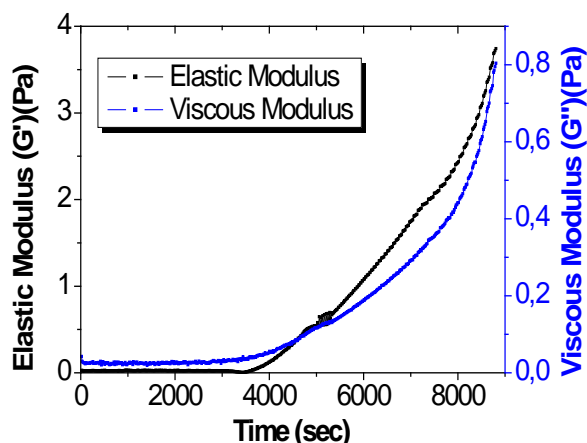
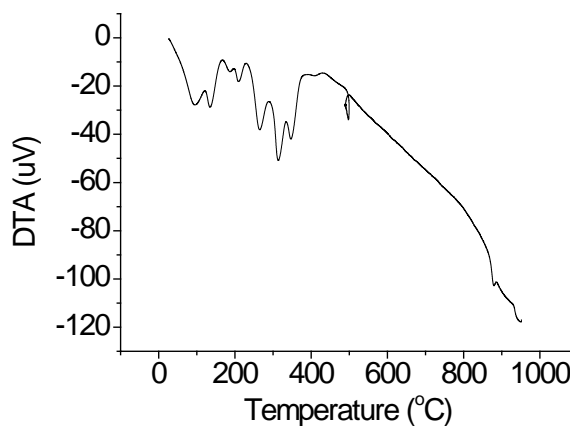
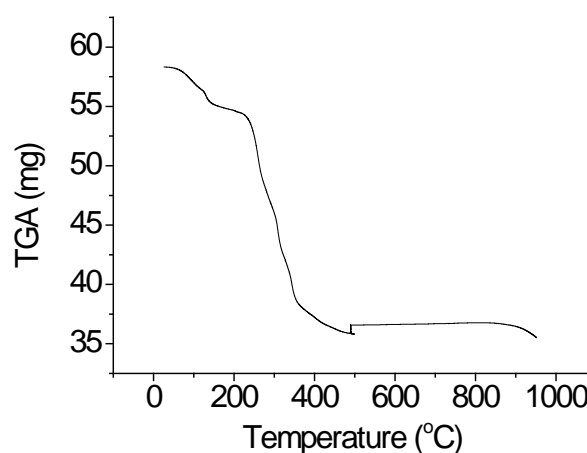


**Figure 2.** The intersection between elastic and viscous modules of the PMN based solutions depending on time and temperature

The most straightforward way to determine heat treatment regime of a process in sol-gel applications is to look at DTA-TGA analysis of the PMN powder xerogel in the temperature range of 25 °C and 1100 °C. Owing to this reason, DTA-TGA curves of the PMN powder xerogel, which were dried from a fresh solution at 25°C for 24 hours in air. As seen in Figure 3a, DTA curves containing dried gel powders are differ from pure perovskite powder. Exothermic and endothermic peaks were found until 400 °C and other thermal effects were not observed above these temperatures until 500 °C. Three thermal phenomena in the xerogel were determined. One of them was the solvent removal at temperature of approximately 130 °C. At this temperature, the endothermic reaction is mostly due to evaporation of physical water, solvent in the gel and carbon based materials coming from alkoxide, solvent and chelating agent burnt out. The second effect was the combustion of OR groups in the samples between 150 and 280 °C. Two exothermic peaks were found at this temperature range. Organic materials coming from Pb, Mg and Nb based precursors, solvent, and chelating agent started to burn out at ~150 °C and the combustion was completed at ~400 °C. The strongest exothermic reaction of the sample took place approximately 370 °C. These reactions caused weight loses with increasing temperature. Approximately, totally weight loss percentage is 42%.



(a)



(b)

**Figure 3.** (a) DTA and (b) TG curve of PMN xerogel heat treated at 150 °C for 30 minutes in air.

Generally speaking, the last stage should have been the formation of ceramic oxides at 500 °C. However, we could not determine oxidation peaks with high intensity in the range of these temperatures. On the contrary, the exothermic peak at 880°C was determined. This peak may responsible for the formation point of perovskite phase or phases.

Another method for determining the heat treatment regime depending on material structure is to investigate how properties of PMN alter in the temperature range of 25 °C and 700 °C with the help of FTIR analysis. In this case, Figure 4 indicates the FTIR absorbance spectra PMN based powders, which were dried 25, 100, 200, 300, 400, 500 and 600 °C for 30 min in air. The spectra show characteristic vibrations in the region of 400–4000  $cm^{-1}$ . The bands at 2800 and 3750  $cm^{-1}$  3600 and

4000  $cm^{-1}$  are due to O-H species in the Pb-Mg-Nb based xerogel, which was heat treated at 25-300 °C, respectively and those at 2200-2500 $cm^{-1}$  is due to C-H stretching frequencies. Notably, a broad band between 3,200 and 4,000  $cm^{-1}$  for all dried and heat treated samples was possible due to residual water present in the samples. The band seen at 1300 and 1500  $cm^{-1}$  is due to C=O arising owing to bridging type metal-acetate bonding (M-OCOO-M). The band at 1444  $cm^{-1}$  is the C-O stretching frequencies and that at 1000  $cm^{-1}$  is due to weakly bound acetic acid molecule (HOOC-R). The spectra of the samples, which was heat treated at 25, 100 and 200 °C were nearly similar. However, the OH band has shifted slightly toward lower frequencies as seen in Figure 6. Upon increasing heat treatment temperature from 25 to 600 °C, the frequencies of O-H, C-H, C=O and M-OCOO-M bands decreased. The spectrum of PMN precursor powders annealed at 500 and 600 °C, which shows an absence of absorption bands corresponding to organics and hydroxyls indicating complete removal of organics and hydroxyls. The common features that appear below 900  $cm^{-1}$  corresponds to the stretching vibrations of Pb=O, Mg=O and Nb=O, and also to the contributions of Pb-O, Mg-O and Nb-O bonds. In the spectrum of 500-600 °C, the band at as 500  $cm^{-1}$  may be assigned to the vibration of PMN bands appear at high temperatures.

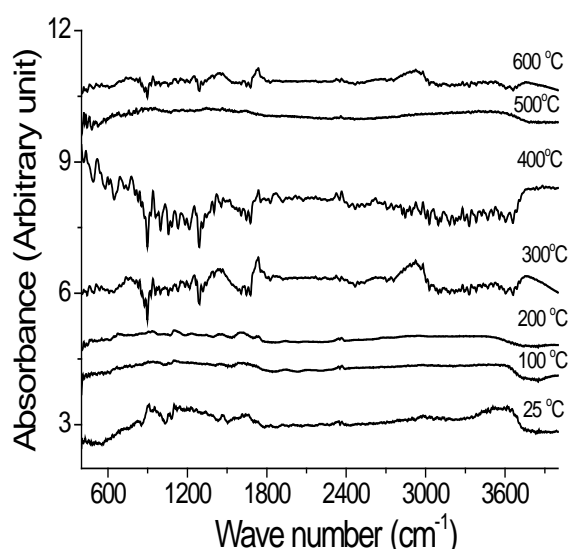


**Figure 4.** FT-IR absorbance spectra of PMN gel samples dried at different temperatures for 30 minutes in air

One of efficient ways to obtain the process optimization is to scan XRD patterns of the PMN powders after DTA-TG and FTIR analysis. XRD patterns of the PMN powders prepared by alkoxide route are presented in Figure 5, showing that the samples were calcined formerly at 500 °C and then sintered at 950 °C and 1100°C for 2 hours. Based on the results, the preliminary experiments seem promising to obtain the perovskite structure.  $Pb(Mg_{0.333}Nb_{0.667})O_3$  phases were found from XRD patterns. It is clear that the intensity of diffraction peaks changed depending on temperatures and maximum perovskite phase was obtained at 950°C.

In Figure 6, XRD patterns of PMN thin films on Si substrate depending on temperature. All of peaks are identified as the diffraction lines  $Pb(Mg_{0.333}Nb_{0.667})O_3$  perovskite and  $Pb_{1.83}Mg_{0.29}Nb_{1.71}O_{6.39}$  pyrochlore phases. This is evidence from Figure 6 that the intensity of PMN and pyrochlore phase peaks showed differences when increasing processing temperature. The XRD pattern clearly showed the random orientations were obtained. In addition, it clearly showed that the peaks at 700°C are optimum phase of perovskite PMN thin film. A consideration of the structural variations accompanying the pyrochlore–perovskite transformation can give insight into how the dielectric constant might be changed from unit cell to unit cell.

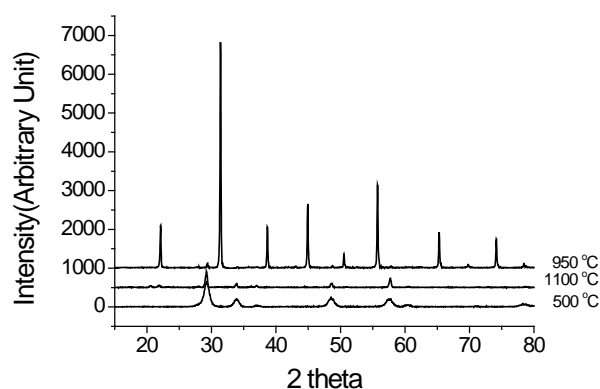


**Figure 5.** XRD results of PMN powders obtained at various temperature.

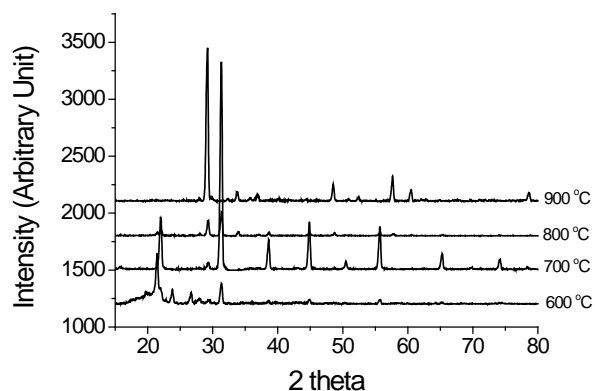
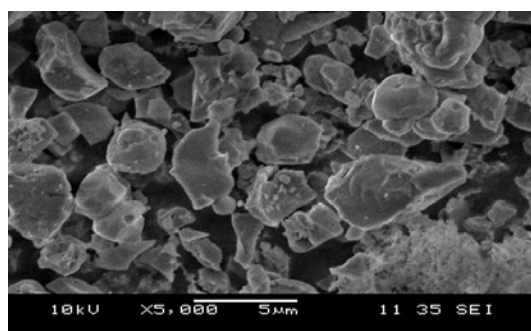
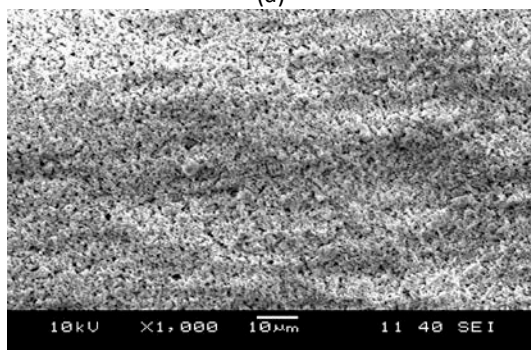


**Figure 6.** XRD results of PMN coatings on n-type Si substrates depending at various temperatures.

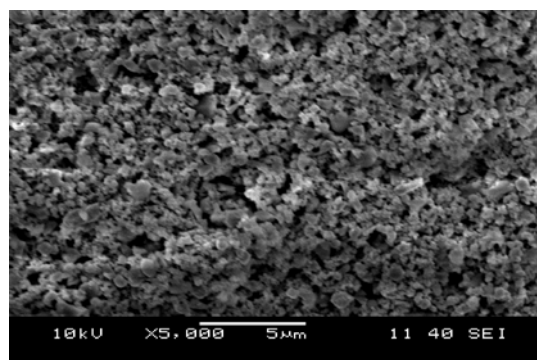
One of the most valuable features of dielectric behaviour is how the microstructure of PMN coatings exhibits. Regarding as the microstructure of PMN coatings, SEM observation was performed. Figure 7 depicts SEM micrographs of PMN on n-type Si substrate. Crack-free but porous and continuous PMN thin film was produced from Pb-Mg-Nb alkoxide precursors. All thin films were coated from powder based solutions after producing PMN powders with different size using sol-gel technique. Figure 7.a depicts SEM micrographs of deposited PMN films using powders prepared before ball milling. SEM examination of PMN shows a porous and having larger particles microstructure on the surface of the substrate.



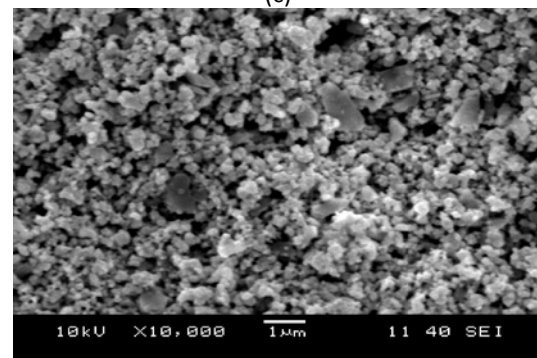
(a)



(b)



(c)



(d)

**Figure 7.** SEM micrographs of PMN thin films on n-type Si substrate (a) 5000x before grinding (b) 1000x (c) 5000x and (d) 10000x after grinding for 12 hours

Figures 7.b, 7.c and 7.d show SEM micrographs of PMN thin films produced from the powder after grinding for 12 hours using zirconia ball milling machine. This structure has also porous morphology but has smaller nano sized particles compared with the coatings in Figure 7.a. Upon comparing with the SEM images of PMN in Figures 7.a and 7.c, it can be pointed out that there is remarkable difference in their surface morphologies because of fabrication method. In this observation, the effect on film morphology of grinding procedure can be easily seen after 12 hours grinding. Figure 7.a reveals the vacancies in coating like coating island on substrate. The vacancies are firstly formed in the coating layers and subsequently independent grain growth corresponding to long uncoated regions between two coating vacancies depending on coating thickness and heating process. The morphologies observed in the different regions of the films can be explained by different particle deposition mechanisms acting during the formation and crystallization of PMN powder as seen in Figure 7.a.

As demonstrated in Figure 7.a, at bottom part of the film, only powder diffusion into the growing film is active. The atom diffusion is limited at the interface with the Si substrate layer and homogeneous growth of PMN crystalline nuclei takes place. At the top of the film, surface diffusion works very fast and only some PMN nuclei are selected for growth, resulting in larger crystallites, which develop in the directions parallel to the film surface. As seen in Figures 7.b, 7.c and 7.d, the same magnification with Figure 7.a, because of grinding with ball milling for 12 hours, coating thickness was decreased and microstructures were changed. As shown from microstructural observations, a regular surface morphology forms as grain size decrease until 200 nm. These thin films are obtained for the coatings, which applied six cycles on Si substrates. Refractive index and film thickness values of PMN films on glass substrate are listed in Table 2. Refractive index and film thickness of PMN films on glass substrates were measured by using spectrophotometer. Refractive index of PMN thin films was 1.522. The film thicknesses of PMN films were determined as 0,960  $\mu\text{m}$  by using measured refractive indexes.

**Table 2.** Refractive index and thickness values of PMN coatings on glass substrates at different temperatures

Annealing temperature ( $^{\circ}\text{C}$ )	Refractive index (nD)	Thickness ( $\mu\text{m}$ )
Before ball milling at		
700	1.5220	1.284
600	1.4034	1.209
700	1.3415	0.960
800	1.3607	0.996

In the study relative permittivity and real capacity ( $C'$ ) of the PMN thin films prepared according to setup in Figure 8 were measured as a function of frequency. It is known that, dielectric constant of PMN is maximum at about  $-10^{\circ}\text{C}$  and above this temperature dielectric constant decrease with increasing temperature. In this work, measurements were performed at room temperature ( $25 \pm 2^{\circ}\text{C}$ ) therefore results do not correspond to the maximum relative permittivity values for these samples. Accordingly, Figure 9.a

describes the relative permittivity,  $\epsilon_r$ , of the PMN samples as a function of frequency. It is obvious that  $\epsilon_r$  of the PMN samples is dependent on the frequency. Relative permittivities of the PMN thin films sintered at  $600^{\circ}\text{C}$ ,  $700^{\circ}\text{C}$  and  $800^{\circ}\text{C}$  were measured to be 5980, 7620 and 1080 at 0.01 Hz, respectively. Similarly, in Figure 9.b, real capacity values of the PMN thin films sintered at  $600^{\circ}\text{C}$ ,  $700^{\circ}\text{C}$  and  $800^{\circ}\text{C}$  is about 0,548, 1,75 and 0,49 nano farad (nF) at 0.01 Hz, respectively. Results showed that under the same conditions  $\epsilon_r$  values of the PMN thin film samples are nearly the same compared to previous thin film studies of PMN films. Previous studies related to the electrical characterization of ferroelectric thick films showed that films may have a lower relative permittivity compared to the bulk ceramics (Deliormanlı, *et.al.* 2007; Sakar-Deliormanli, *et.al.* 2008). For instance, Gentil, *et.al.* (2004) measured the relative permittivity of PMN films as 10,000 at 0.1 kHz which is lower than the values of the bulk ceramics (17,800 at 0.1 kHz) under the same conditions. They also found that the decrease of film thickness lead to the decrease of dielectric properties. In this study the lower relative permittivity values in PMN thin films compared to the previous thin film studies may be attributed to the several factors, including higher porosity and higher roughness.

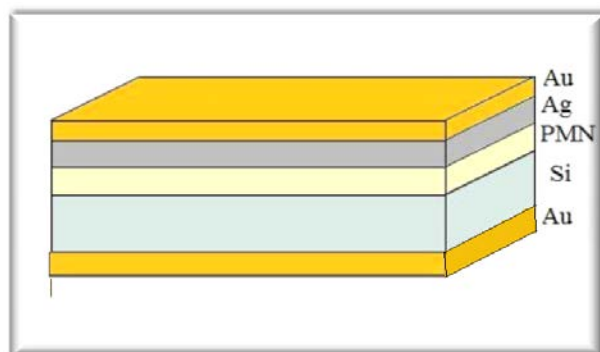


**Figure 8.** Electrical measurement setup of the samples prepared as a Metal-Oxide-Semiconductor (MOS) structure



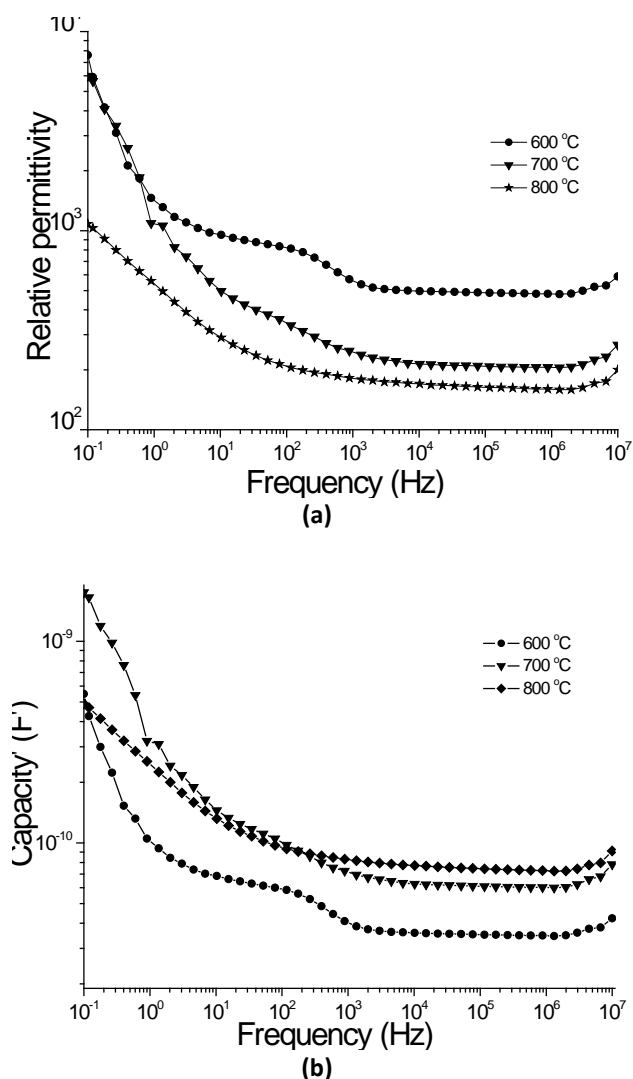


**Figure 9.** (a) Relative dielectric constant and (b) capacity values of the PMN coatings on Si as a function of frequency (Hz) at 25 °C for different temperatures.

#### 4. Conclusion

PMN based thin films were synthesized on Si substrate from the sol-gel derived PMN powders obtained the solutions prepared from Pb, Mg and Nb based precursors, methanol and GAA for thin film capacitor applications. The following results are below:

1) Turbidity value of the solutions was measured as 8,42 ntu. Acidity of the solutions does not change with in first 15 minutes because it stabilizes. In solution characterization, viscosity, viscous and elastic modulus of the solutions as a function of time were found to be  $2.6 \times 10^{-2}$  Pa.s,  $1.2 \times 10^{-2}$  Pa.s and  $4 \times 10^{-3}$  Pa.s at 25°C, 50°C and 80 °C for 9000 s

in air, respectively. Gel point of the solution occurred at 4703 s.

2) The first thermal phenomenon was the solvent removal at temperature of approximately 130 °C. The second phenomenon was combustion of OR groups at temperatures between 150 and 280 °C. The third and fourth stages were the formations of oxide layer structure at 500 °C. The exothermic reaction was occurred at 880 °C. This may be responsible for the formation point of perovskite phase. A weight loss of the xerogel sample is about 42% for temperatures from 25 up to 950 °C.

3) Depending on these temperatures, the structures of the films were changed as explained in FTIR results. The spectra of the samples, which were heat treated at 25 and 200 °C were nearly similar. In the spectrum of 500-600 °C, the band at  $500 \text{ cm}^{-1}$  may be assigned to the vibration of PMN bands appear at high temperatures.

4)  $Pb(Mg_{0.333}Nb_{0.667})O_3$  PMN perovskite phases were formed at 950°C. It is clear that the peaks at 700°C are optimum phase of perovskite PMN thin films.

5) In microstructural observation, crack-free but porous and continuous PMN thin film was produced from Pb-Mg-Nb alkoxides precursors. After grinding for 12 hours using zirconia ball milling machine, these structures have also porous morphology but has smaller nano sized particles then before grinding microstructure on the surface.

6) Refractive index and thickness of PMN thin films were found to be 1,3415 and 0,960 at 700 °C, respectively. Relative permittivities of the PMN thin films sintered at 600 °C, 700 °C and 800 °C were measured to be 5980, 7620 and 1080 at 0.01 Hz, respectively. The lower relative permittivity values in PMN thin films compared to the previous thin film studies may be attributed to the several factors, including higher porosity and higher roughness.

## Acknowledgements

This work was supported by State Planning Foundation (DPT) and we specially thank to Mr. Safhak Turan for helping in this study.

## References

- Bhuiyan, M.S., Paranthaman, M. and Salama, K., 2006. Topical review: solution-derived textured oxide thin films-a review. *Superconductor Science and Technology*, **19**, R1-R21.
- Chaipanich, A. and Tunkasiri, T., 2007. Effect of milling time on the properties of  $Pb(Mg_{1/3}Nb_{2/3})O_3$  ceramics using the starting precursors  $PbO$  and  $MgNb_2O_6$ . *Current Applied Physics*, **7**, 281-284.
- Culha, O., Ebeođlugil, M.F., Birlik, I., Celik, E. and Toparli, M., 2009. Synthesis and characterization of semiconductor tin oxide thin films on glass substrate by sol-gel technique. *J. Sol-Gel Science and Technology*, **5**, 32-41.
- Deliormanlı, A.M. Celik, E. and Polat, M., 2007. The isoelectric point of lead magnesium niobate. *J. Am. Ceram. Soc.*, **90**, 3314-3317.
- Gentil, S., Damjanović D. and Setter, N., 2004.  $Pb(Mg_{1/3}Nb_{2/3})O_3$  and  $(1-x) Pb(Mg_{1/3}Nb_{2/3})O_3-xPbTiO_3$  relaxor ferroelectric thick films: processing and electrical characterization. *J. Electroceram.*, **12**, 151-161.
- Guha, J.P., 1999. Reaction chemistry and subsolidus phase equilibria in lead-based relaxor systems: Part I Formation and stability of the perovskite and pyrochlore compounds in the system  $PbO-MgO-Nb_2O_5$ . *J. Materials Science*, **34**, 4985- 4994.
- Parola, S.;et al., 2003. New sol-gel route for processing of PMN thin films. *J. Sol-Gel Science and Technology*, **26**, 1109-1112.
- Pierre, A.C. and Bernard-Lyon I., 1998. Introduction to sol- gel processing. University Claude, Kluwer Academic Publishers-Boston, Dordrecht, London, pp. 186-190.
- Schwartz, R.W., 1997. Chemical solution deposition of perovskite thin films. *Chem. Mater.*, **9**, 2325-2340.
- Sakar-Deliormanli, A., Celik, E. and Polat, M., 2008. Phase formation and microstructure of  $Nd^{+3}$  doped  $Pb(Mg_{1/3}Nb_{2/3})O_3$  prepared by sol-gel method. *J. Mater Sci, Mater Electron*, **19**, 577-583.
- Sakar-Deliormanli, A., Celik, E. and Polat, M., 2009. Preparation of the  $Pb(Mg_{1/3}Nb_{2/3})O_3$  films by aqueous tape casting. *J. the European Ceramic Society*, **29**, 115-123.